

REVISITING HALLUCINATION DETECTION WITH EFFECTIVE RANK-BASED UNCERTAINTY

Rui Wang¹ Zeming Wei¹ Guanzhang Yue¹ Meng Sun¹

¹Peking University

ABSTRACT

Detecting hallucinations in large language models (LLMs) remains a fundamental challenge for their trustworthy deployment. Going beyond basic uncertainty-driven hallucination detection frameworks, we propose a simple yet powerful method that quantifies uncertainty by measuring the effective rank of hidden states derived from multiple model outputs and different layers. Grounded in the spectral analysis of representations, our approach provides interpretable insights into the model’s internal reasoning process through semantic variations, while requiring no extra knowledge or additional modules, thus offering a combination of theoretical elegance and practical efficiency. Meanwhile, we theoretically demonstrate the necessity of quantifying uncertainty both internally (representations of a single response) and externally (different responses), providing a justification for using representations among different layers and responses from LLMs to detect hallucinations. Extensive experiments demonstrate that our method effectively detects hallucinations and generalizes robustly across various scenarios, contributing to a new paradigm of hallucination detection for LLM truthfulness.

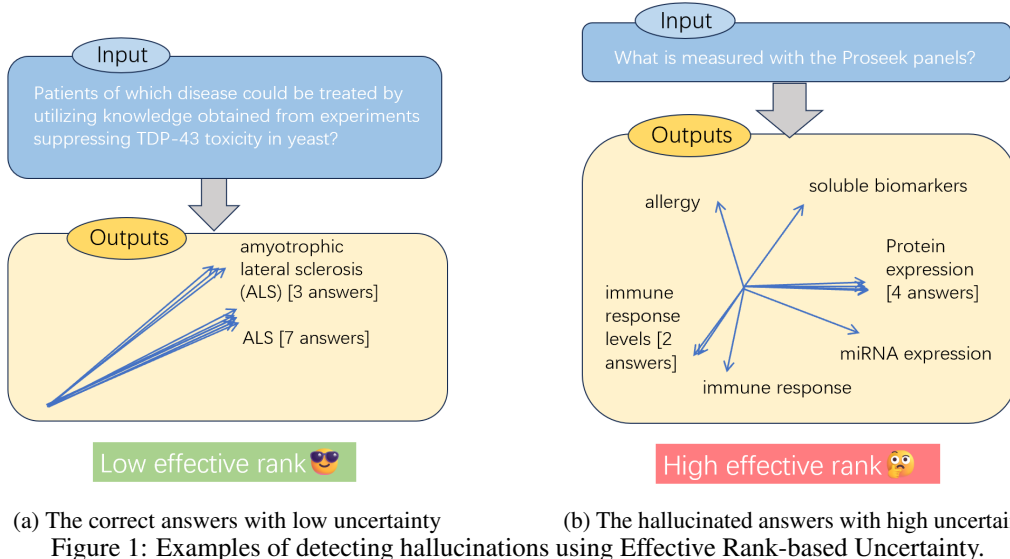
1 INTRODUCTION

The advent of Large Language Models (LLMs) has catalyzed a paradigm shift across artificial intelligence, enabling remarkable capabilities in generative and reasoning tasks. From sophisticated dialogue to complex code generation, their prowess is undeniable (Achiam et al., 2023; Team et al., 2023). However, their reliability continues to suffer from **hallucinations** (Huang et al., 2025), where models produce outputs that are fluent and contextually plausible, but factually incorrect. Unlike simple errors, hallucinations are particularly insidious because they are often indistinguishable from trustworthy responses, making them especially dangerous in high-stakes domains such as healthcare and scientific discovery. The issue arises from the probabilistic nature of next-token prediction: LLMs optimize for linguistic plausibility rather than factual accuracy, and without explicit grounding, minor biases or gaps in knowledge can cascade into confident yet misleading narratives. As a result, hallucinations not only limit practical deployment but also raise fundamental questions about the epistemic reliability of generative models.

Despite various attempts to mitigate hallucinations through architectural modifications and training heuristics, the issue remains far from solved. The challenge of mitigating hallucinations is intrinsically tied to the problem of **uncertainty quantification (UQ)**. Ideally, an LLM should not only provide an answer but also communicate how confident it is. If a model could reliably estimate its epistemic uncertainty, it could abstain or defer when unsure, thereby reducing hallucinations (Kendall & Gal, 2017; Abbasi Yadkori et al., 2024). Although a large body of research has explored UQ in traditional machine learning, existing methods such as Monte Carlo dropout (Gal & Ghahramani, 2016) or deep ensembles (Lakshminarayanan et al., 2017) are computationally impractical for billion-parameter LLMs. Similarly, approaches based on retrieval augmentation or auxiliary calibration modules add system complexity and latency. This highlights the pressing need for lightweight, self-contained, and scalable UQ techniques tailored to the architecture and deployment constraints of modern LLMs.

In this paper, we propose an **internally interpretable** solution for UQ that operates purely from the internal state of the model. Our hypothesis is that the internal representations of LLMs contain rich but underutilized information. These representations not only reveal the model’s reasoning

process, enhancing internal interpretability, but their sampling probability distributions also capture different reasoning paths, which in turn manifest as semantic divergences. Intuitively, since LLMs inherently involve stochasticity during forward propagation, small probabilistic perturbations can lead to noticeable shifts in their generation process. When a model lacks sufficient knowledge or reasoning ability, these perturbations can cause its internal representations to diverge semantically during layer-wise forward passes and eventually surface as hallucinations (Huang et al., 2025). In contrast, a confident and well-grounded model maintains robust and constrained hidden trajectories despite such perturbations, leading to consistent and reliable output. Thus, representational divergence provides a natural signal for quantifying uncertainty and identifying hallucination-prone generations.



To formalize this intuition, we leverage the notion of **effective rank** (Roy & Vetterli, 2007) of the matrix of embedding vectors as a measure of uncertainty. Effective rank serves as a smooth measure of the divergence among vectors within a matrix, and is employed in our method to detect semantic variations in different embedding vectors. Intuitively, a low effective rank indicates that the activation energy is concentrated in a few directions, suggesting a confident, deterministic internal state (Figure 1a). By contrast, a high effective rank signals that the energy is spread diffusely, indicative of uncertainty, confusion, and a higher likelihood of hallucination (Figure 1b).

We extensively validate our hypothesis across multiple benchmark datasets and model architectures. Our experiments demonstrate that effective rank is a highly predictive signal for hallucination detection, consistently outperforming or matching the performance of established strong baselines while being significantly efficient and scalable. Additionally, we demonstrate how aleatoric uncertainty (the inherent stochasticity of LLMs) progressively amplifies and obscures epistemic uncertainty (uncertainty in the knowledge and capabilities encoded by the model’s parameters) within the model’s internal representations during a single sequence generation without multiple samples. This finding provides both the theoretical justification for the necessity of semantic sampling through multiple responses and the foundational rationale for its effectiveness.

Our contributions are threefold:

- **A Novel Spectral Perspective on Uncertainty.** We propose and empirically validate the Effective Rank-based Uncertainty as an efficient, robust, and model-intrinsic measure of uncertainty for LLMs.
- **A lightweight, Training-Free Detector.** We introduce a rapid hallucination detection method that does not require additional tools, fine-tuning, or external knowledge.
- **Practical and Theoretical Analysis.** We conducted experiments across different scenarios, demonstrating the consistent effectiveness of our method and providing interpretable insights for the quantitative analysis of uncertainty within the model’s internal representations.

2 RELATED WORK

2.1 HALLUCINATION DETECTION

Hallucination in LLMs has been widely studied from multiple perspectives. A major line of work attributes hallucinations to various forms of uncertainty inherent in the model. Specifically, hallucinations often arise due to (i) insufficient or incomplete knowledge and reasoning capabilities, (ii) excessive stochasticity in the generation process, and (iii) low faithfulness to the provided context. These uncertainty-related factors account for a large proportion of hallucination cases in practice (Huang et al., 2025; Zhang et al., 2025; Tonmoy et al., 2024). However, hallucinations can also occur even when model uncertainty is low, for example, when the model’s internal knowledge itself is systematically incorrect or outdated. Such cases typically require techniques like knowledge editing or targeted fine-tuning for correction (Huang et al., 2024).

To correct and reduce hallucinations in LLMs, we first need highly accurate hallucination detection methods. Methods for detecting hallucinations in LLMs generally fall into three main categories. Retrieval-based methods verify generated content against external knowledge sources or retrieved evidence (Lewis et al., 2020). Self-verification approaches such as P_False (Kadavath et al., 2022) and SelfCheckGPT (Manakul et al., 2023) prompt the model to evaluate its own generations for consistency or correctness. Supervised detection involves training classifiers on labeled datasets to identify hallucinated content (Arteaga et al., 2024). While often effective, these methods typically depend on external tools or costly annotations, and may introduce latency for real-time applications. These limitations motivate the exploration of intrinsic, uncertainty-based detection paradigms.

2.2 UNCERTAINTY QUANTIFICATION FOR HALLUCINATION DETECTION

Uncertainty estimation has emerged as a prominent approach for hallucination detection in LLMs. The core premise is that a model’s internal confidence can indicate output veracity. Initial approaches used token-level or sequence-level probability distributions, such as the **Length-normalized Entropy** (Malinin & Gales, 2020), which normalizes entropy by the number of tokens to mitigate the impact of varying sequence lengths. However, these methods capture lexical rather than semantic uncertainty. As models can be lexically confident yet semantically incorrect (Kuhn et al., 2023), recent benchmarks (Ye et al., 2024; Nado et al., 2021) have spurred exploration of semantic properties and internal representations for improved detection.

Based on semantic analysis, Kuhn et al. (2023); Farquhar et al. (2024) introduced **Semantic Entropy** (SE) and **Discrete Semantic Entropy** (DSE) to address limitations of token-level metrics. SE and DSE cluster generations by semantic equivalence using natural language inference (NLI) models, then compute entropy over the distribution of semantic categories. Note that while DSE directly estimates the probability of each semantic category using the frequency of answers in each cluster, SE further incorporates a token-level probability adjustment. High SE indicates semantic uncertainty, effectively capturing meaning-level variations. Meanwhile, the INSIDE framework proposed by Chen et al. (2024) measures the model’s internal uncertainty by extracting the internal embedding vectors of the model, computing their covariance matrix, and calculating the determinant of the covariance matrix through eigenvalue decomposition to obtain the **Eigenscore**. This Eigenscore approximates *differential entropy*, with higher scores indicating internal inconsistency. These methods each delve deeply into the uncertainty about semantic variances or internal representations, but the relationship between internal representations and external semantic information remains largely unexplored.

3 METHODOLOGY

In this section, we propose a novel uncertainty-based approach to hallucination detection in LLMs. Our primary motivation is to additionally leverage the internal representations of the model to measure its uncertainty, and we adopt the effective rank from spectral analysis as our main method, which integrates the characteristics of smoothness and clear practical interpretability. This section introduces the procedure and the underlying theoretical justification.

3.1 CONSTRUCTING THE EMBEDDING MATRIX

For each query q , we first construct the representation matrix extracted from different layers and responses to calculate the effective rank. To this end, we sample m_1 responses and extract embeddings from m_2 layers per response, resulting in $m = m_1 \times m_2$ embedding vectors $\vec{a}_1, \vec{a}_2, \dots, \vec{a}_m \in \mathbb{R}^n$. These vectors are concatenated into a representation matrix:

$$A = [\vec{a}_1, \vec{a}_2, \dots, \vec{a}_m] \in \mathbb{R}^{n \times m} \quad (1)$$

where each \vec{a}_i corresponds to the embedding of a particular response at a specific layer. Following [Skean et al. \(2025\)](#), who find that intermediate layers of an LLM strike the best balance between preserving useful information and removing noise, while the final layer often overfits the training objective and eliminates generalization, we therefore extract the embedding vector from the exact middle hidden layer for every response, both in our method and the Eigenscore baseline.

3.2 SPECTRAL ANALYSIS

Next, we want to quantify the dispersion of the column vectors of this matrix, and the notion of singular values offers a perfectly suited mathematical tool for this, since singular values measure how much the matrix stretches or compresses vectors along certain directions in space. We then compute the singular value decomposition (SVD) of the matrix:

$$A = U\Sigma V^\top \quad (2)$$

where $\Sigma = \text{diag}(\sigma_1, \sigma_2, \dots, \sigma_m)$ contains the singular values in descending order.

To quantify the dispersion of vectors across different directions using the entropy of the singular values, we normalize the singular value spectrum into a probability distribution:

$$p_i = \frac{\sigma_i}{\sum_{j=1}^m \sigma_j}, \quad i = 1, \dots, m \quad (3)$$

3.3 ENTROPY-BASED MEASURE AND EFFECTIVE RANK

We consider the Shannon entropy of the singular value distribution as our measure of uncertainty for the query q :

$$H = - \sum_{i=1}^m p_i \ln p_i \quad (4)$$

Using entropy to quantify uncertainty is common, yet our approach rests on an exceptionally clear and elegant mathematical foundation. The quantity $\exp(H)$ is the *effective rank* of the matrix A , which measures the “effective linear independence” of the vectors in matrix A ([Roy & Vetterli, 2007](#)). Intuitively, $\exp(H)$ corresponds to the effective number of distinct semantic modes represented in the embedding vectors. Hence, a larger entropy indicates higher uncertainty in the model’s outputs.

Through Jensen’s inequality, it can be readily shown that the effective rank of a matrix equals its true rank if and only if the matrix has a rank of 1 or its column vectors are pairwise orthogonal and of equal length (corresponding to the cases of minimum and maximum uncertainty, respectively). In all other cases, the effective rank is strictly less than the true rank and varies continuously with the dispersion of the vectors. Therefore, effective rank smoothly encodes how divergent the column vectors are. In practice, semantically similar embedding vectors are often similar yet not perfectly aligned, so a continuous effective rank captures their consistency far better than the discrete true rank. Moreover, the effective rank here possesses a clear and practical interpretation as the “effective number of semantic categories”, providing us with an excellent tool for further analyzing and enhancing the internal interpretability of LLM models ([Zhuo et al., 2023](#)).

We summarize the above procedure for computing the effective rank in Algorithm 1. In the following section, we will empirically validate the effectiveness, robustness and generality of this method.

Algorithm 1: Effective Rank-based Uncertainty Computation

Input: Query q , number of responses m_1 , number of layers per response m_2 , LLM (white-box)
Output: Effective rank $\exp(H)$

for $i : 1 \rightarrow m_1$ (*in parallel*) **do**

- | Sample response r_i from the LLM using query q ;
- | Extract the hidden state h_i corresponding to the last generated token of response r_i ;
- | **for** $j : 1 \rightarrow m_2$ (*in parallel*) **do**
- | | Extract embedding vector $\mathbf{a}_{ij} \in \mathbb{R}^n$ from the corresponding position of h_i
- | | **end**
- | **end**

Form embedding matrix $A = [\mathbf{a}_{11}, \dots, \mathbf{a}_{1m_2}, \dots, \mathbf{a}_{m_1m_2}] \in \mathbb{R}^{n \times m}$, where $m = m_1 \times m_2$;

Compute SVD: $A = U\Sigma V^\top$, with singular values $\{\sigma_1, \dots, \sigma_m\}$;

Normalize singular values: $p_i = \sigma_i / \sum_{j=1}^m \sigma_j$ for $i = 1, \dots, m$;

Compute entropy: $H = -\sum_{i=1}^m p_i \ln p_i$;

return $\exp(H)$

4 EXPERIMENTS

4.1 EXPERIMENTAL SETUP

Datasets. Our dataset selection is designed to rigorously evaluate hallucination detection across a spectrum of knowledge and reasoning domains. TriviaQA (Joshi et al., 2017) serves as a broad open-domain knowledge benchmark. In contrast, Natural Questions (NQ) (Kwiatkowski et al., 2019) and BioASQ (Tsatsaronis et al., 2015) probe deeper into specialized knowledge within natural science and healthcare domains where LLM hallucinations can be particularly misleading and harmful. To test foundational competencies beyond factual recall, we also include SQuAD (Rajpurkar et al., 2016) for context understanding and text inference.

Models. For our backbone language models, we utilize three widely recognized open-weight models: Llama-2-7b-chat (Touvron et al., 2023), Llama-2-13b-chat, and Mistral-7B-v0.1 (Jiang et al., 2023) to evaluate our methods across models of varying scales and distinct architectural lineages.

Evaluation Metrics. To determine whether a model’s generation contains hallucinations, we use **ROUGE-L** (Lin, 2004), an n-gram based metric that computes the longest common subsequence between the generation and the ground-truth answer. A generation is considered correct if its ROUGE-L score ≥ 0.5 ; otherwise, it is flagged as a hallucination. The validity of this annotation method is discussed in Appendix F. To evaluate the overall performance of the hallucination detection methods themselves, we use the **Area Under the Receiver Operating Characteristic curve (AUROC)** (Filos et al., 2019). AUROC is chosen as it provides a comprehensive measure that is agnostic to the absolute scale of the uncertainty scores produced by different detectors. This makes it an ideal metric for comparing the ability to rank hallucinated examples higher than non-hallucinated ones.

Baselines. We benchmark our proposed method against recent strong baselines: **Semantic Entropy**, **Discrete Semantic Entropy** (Farquhar et al., 2024), and **Eigenscore** (Chen et al., 2024). We have also considered these representative baselines: **P_False** (Kadavath et al., 2022), and **Length-Normalized Entropy** (Malinin & Gales, 2020). Detailed introductions to these baselines can be found in Section 2.

Implementation Details. All experiments were conducted on a virtual GPU (vGPU) with 48GB of memory. We use a temperature of 1.0 for sampling and generate $N = 10$ answers per input. For embedding extraction, we utilize the hidden state of the last token from the exact middle layer of the model. Finally, in the Eigenscore calculation, we follow the recommendation of Chen et al. (2024) and set the small regularization term to $\alpha = 0.001$.

4.2 MAIN RESULTS

The overall performance comparison of our Effective Rank (ER) method against five baselines is summarized in Table 1. The results, measured in AUROC across three models and five diverse datasets, demonstrate the efficacy and generality of our approach in detecting hallucinations.

Model	Dataset	ER (Ours)	ES	PF	DSE	LNE	SE
Llama-7b	TriviaQA	0.7877	0.7802	0.6625	0.7758	0.6947	0.7750
	SQuAD	0.7212	0.7199	0.6594	0.7172	0.6505	0.7181
	BioASQ	0.8447	0.8433	0.7321	0.8437	0.4703	0.8425
	NQ	0.7029	0.7056	0.6584	0.6984	0.6495	0.7001
Average		0.7641	0.7623	0.6781	0.7588	0.6163	0.7589
Llama-13b	TriviaQA	0.7407	0.7342	0.7379	0.7331	0.6930	0.7390
	SQuAD	0.7259	0.7239	0.6945	0.7381	0.6886	0.7350
	BioASQ	0.8234	0.8215	0.7980	0.7951	0.5610	0.7988
	NQ	0.7284	0.7270	0.6841	0.7234	0.6866	0.7258
Average		0.7546	0.7517	0.7286	0.7474	0.6573	0.7497
Mistral-7b	TriviaQA	0.7634	0.7579	0.7239	0.7575	0.6519	0.7553
	SQuAD	0.7208	0.7120	0.6333	0.7227	0.6223	0.7238
	BioASQ	0.8563	0.8513	0.7173	0.8507	0.5955	0.8513
	NQ	0.7658	0.7627	0.7523	0.7678	0.6770	0.7662
Average		0.7766	0.7710	0.7067	0.7747	0.6367	0.7742

Table 1: Overall comparison of ER with baselines, where ER denotes Effective Rank, ES denotes Eigenscore, PF denotes P_False, DSE denotes Discrete Semantic Entropy, LNE denotes Length-Normalized Entropy, and SE denotes Semantic Entropy. All numbers in the table are AUROC scores; values closer to 1 indicate stronger hallucination-detection ability.

Overall Effectiveness. Our method achieves the highest AUROC score in 8 out of 12 evaluation scenarios, establishing a consistent and strong performance baseline. Notably, this superiority is not confined to a specific model or dataset but is observed across various scales (7b and 13b parameters) and architectures (Llama and Mistral). This indicates that the principle of analyzing representation space stability through effective rank is a generalizable strategy for hallucination detection. Even in cases where ER does not rank first, its performance remains highly competitive (e.g., on NQ dataset). We also note that our method’s overall margin over the baselines is larger on Llama-2-13B-chat than on Llama-2-7B-chat, suggesting its potential scales with model size.

Analysis of Shortcomings. A primary limitation of our method is observed in its unstable performance on the SQuAD dataset. This suggests that for tasks requiring complex textual reasoning and comprehension, rather than pure factual recall, the relationship between internal representations and uncertainty may be less consistent. In such scenarios, SE and DSE methods, which directly measure semantic variation across multiple sampled answers, appear to capture uncertainty more reliably. Nevertheless, Effective Rank remains highly competitive compared to all methods except SE and DSE on SQuAD dataset. Our ablation study further analyzes the interplay between the roles of different hidden layers and the requirements of tasks across various datasets.

Comparative Analysis of Baselines. The results also shed light on the relative performance of existing methods. The Eigenscore method, apart from showing a noticeable gap compared to Effective Rank on the TriviaQA dataset, remains relatively close to our approach and occasionally even surpasses it by a narrow margin. This is because both methods utilize the representations from the model’s internal hidden layers to measure uncertainty. However, Eigenscore is an approximation of differential entropy, whereas Effective Rank directly yields an intuitive and effective uncertainty indicator, the “effective number of distinct semantic categories”. This gives Effective Rank an overall advantage over Eigenscore. Although SE and DSE methods generally perform better than our approach on SQuAD, they require an auxiliary NLI model and additional time for semantic reasoning (Table 2). Additionally, while P_False and LNE methods are relatively unstable, they occasionally deliver relatively strong performance.

In conclusion, the main results strongly support the effectiveness of our Effective Rank approach. Its dominant performance on TriviaQA and BioASQ tasks highlights its value as a tool for detecting factual hallucinations, a critical challenge for modern LLMs.

Methods	Effective	Internally interpretable	Semantic Information	Time Efficiency
ES	✓	✓	✗	9.5s
SE, DSE	✓	✗	✓	11.7s
PF	✗	✗	✗	10.1s
LNE	✗	✗	✗	9.6s
ER (ours)	✓	✓	✓	9.5s

Table 2: Qualitative comparison of hallucination detection methods. In terms of time efficiency, the numbers in the table indicate the average time spent on each question in the experiment where each method generated results for 3 models \times 4 datasets under the parameter settings of the main experiment. Our method took an average of 9.5 seconds, which is essentially the same as the time required to naturally generate answers without hallucination detection. The detailed time complexity analysis of our ER method can be found in Appendix F.

4.3 ABLATION STUDIES

N	Dataset	M1	M5	L1	L5	Best Baseline
10	TriviaQA	0.7877	0.7700	0.7809	0.7629	0.7802 (ES)
	SQuAD	0.7212	0.7217	0.7191	0.7190	0.7199 (ES)
	BioASQ	0.8447	0.8461	0.8481	0.8472	0.8437 (DSE)
	NQ	0.7029	0.7038	0.7036	0.7049	0.7056 (ES)
	Average	0.7641	0.7604	0.7629	0.7585	0.7623 (ES)
15	TriviaQA	0.7862	0.7902	0.7870	0.7807	0.7825 (ES)
	SQuAD	0.7407	0.7407	0.7391	0.7395	0.7391 (ES)
	BioASQ	0.8715	0.8690	0.8684	0.8678	0.8682 (ES)
	NQ	0.7182	0.7166	0.7174	0.7188	0.7206 (ES)
	Average	0.7792	0.7780	0.7767	0.7791	0.7776 (ES)
20	TriviaQA	0.7786	0.7780	0.7729	0.7702	0.7743 (ES)
	SQuAD	0.7596	0.7604	0.7599	0.7610	0.7588 (DSE)
	BioASQ	0.8645	0.8625	0.8638	0.8620	0.8628 (ES)
	NQ	0.7277	0.7292	0.7274	0.7278	0.7284 (ES)
	Average	0.7826	0.7825	0.7810	0.7803	0.7809 (ES)

Table 3: Ablation studies on Llama-2-7b-chat, where N refers to the number of generations, M1 refers to extracting the exact middle hidden layer for each answer in the ER method (i.e., the ER method used in the main experiment), M5 refers to extracting the middle five layers, L1 refers to extracting the last layer, and L5 refers to extracting the last five layers. Ablation studies on other models and complete experimental data can be found in Appendix D.

Number of generations and the use of different hidden layers. Our ablation studies on Llama-2-7b-chat reveal that the performance of the ER method is robust to the number of generations, since it maintains a consistent overall advantage over the baselines across different values of N. Moreover, no single layer extraction strategy consistently outperforms all others, indicating a complex interaction between the task domain and the representational properties of different model layers. Notably, although M5, L1, and L5 hidden layer selection strategies yield results comparable to M1 and can complement M1 to a certain extent, they are slightly inferior overall and exhibit marginally less stability (somewhat analogous to how DSE is generally slightly weaker than SE). Furthermore, increasing the number of generations (N) does not yield uniform improvements, implying a task-dependent optimum exists for this hyperparameter.

Temperature. According to Table 4, we observe that the hallucination detection performance is generally optimal when the temperature is set around 0.5 and 1.0. Under these conditions, our Effective Rank method also demonstrates a significant overall advantage. Excessively high or low temperatures substantially undermine uncertainty-based hallucination detection methods, while the Self-Verification-based P_False method unexpectedly exhibits a notable relative advantage in such

		TriviaQA	SQuAD	BioASQ	NQ	Average
t=0.1	Best ER	0.6782 (L1)	0.6466 (M5)	0.7416 (L5)	0.6841 (L1)	0.6768 (L1)
	Best Baseline	0.6695 (PF)	0.6413 (PF)	0.7720 (PF)	0.7308 (PF)	0.7034 (PF)
t=0.5	Best ER	0.7628 (M5)	0.7401 (L5)	0.8452 (L5)	0.7724 (L1)	0.7771 (L1)
	Best Baseline	0.7350 (ES)	0.7330 (ES)	0.8378 (ES)	0.7641 (ES)	0.7675 (ES)
t=1.0	Best ER	0.7651 (L1)	0.7208 (M1)	0.8584 (M5)	0.7696 (M5)	0.7769 (M5)
	Best Baseline	0.7579 (ES)	0.7268 (SE)	0.8513 (ES)	0.7678 (DSE)	0.7747 (DSE)
t=2.0	Best ER	0.6685 (M5)	0.5754 (M1)	0.7329 (M5)	0.6118 (M1)	0.6437 (M1)
	Best Baseline	0.7084 (PF)	0.5698 (ES)	0.7244 (SE)	0.7006 (PF)	0.6640 (PF)

Table 4: Ablation studies on Mistral-7B-v0.1 about temperature, where t denotes the temperature, and Best ER refers to the Effective Rank that performed the best among the four hidden vector selection methods (M1, M5, L1, L5). Complete experimental data can be found in Appendix D.

scenarios, albeit with remaining instability. Moreover, the detailed data show that the L1 and L5 methods are more robust to low temperatures, while the M1 and M5 methods are more robust to high temperatures.

5 INTERNAL INTERPRETABILITY: THE DECOMPOSITION AND QUANTITATIVE ANALYSIS OF UNCERTAINTY

5.1 EMPIRICAL MOTIVATION

While multi-sample methods are effective for hallucination detection, we still want to explore the real-time detection without multiple samples. On Llama-2-7b-chat, we use a sliding window to measure the effective rank of the internal representations across every three consecutive layers and then take the average. The final results vary slightly between different responses, but generally fluctuate around 1.9. This indicates that semantic changes occur within the model during the reasoning process, and these shifts exhibit a certain degree of similarity but little variability between different responses. This finding is broadly consistent with conclusions drawn from using cosine similarity of internal representations to assess internal consistency (Min et al., 2024). However, the experiments revealed that this form of internal uncertainty showed only a weak correlation with hallucinations (overall AUROC ≈ 0.57 , barely exceeding the random chance). This unsuccessful attempt prompted us to reconsider: *What truly constitutes effective internal uncertainty for hallucination detection?*

According to the perspective of Depeweg et al. (2018), the uncertainty in the predictions of Deep Neural Networks can be decomposed into two primary types: *aleatoric uncertainty*, which is inherent in the data and model architecture due to its ambiguity or inherent stochasticity, and *epistemic uncertainty*, which stems from the model’s lack of knowledge or ability. The latter is considered particularly critical for detecting hallucinations. We subsequently argue, however, that within any single sampled response, the information signal pertaining to epistemic uncertainty is largely masked by aleatoric uncertainty. Furthermore, this aleatoric uncertainty can propagate and become amplified through the model’s reasoning process. Consequently, when the LLM’s internal knowledge is insufficient to produce a determinate result amidst this prevailing uncertainty noise (i.e., when a hallucination occurs), the generation and reasoning processes of LLMs often involve probabilistic distributions with obvious uncertainty, which ultimately manifest as semantic divergences across different sampled answers (Manakul et al., 2023; Huang et al., 2025).

5.2 PRELIMINARIES AND PROBLEM SETUP

Consider an autoregressive language model parameterized by θ . Given an input prompt q , the model generates a sequence of tokens (y_1, y_2, \dots, y_T) and a corresponding sequence of hidden states (h_1, h_2, \dots, h_L) , where $h_t \in \mathbb{R}^d$ is the hidden state at step t . The generation process is defined as:

$$y_t \sim p(y_t | h_{t-1}; \theta), \quad h_t = f(h_{t-1}, y_t; \theta)$$

where f is a deterministic, non-linear transformation, and p is the model’s output distribution.

To frame our discussion, we adapt the Bayesian deep learning framework (Kendall & Gal, 2017; Depeweg et al., 2018) to reason about the hidden states. We consider the expected total variance of the hidden state h_t across the data generation process, which can be decomposed into two components:

$$\underbrace{\text{Var}(h_t)}_{\text{Total Uncertainty}} = \underbrace{\mathbb{E}_\theta[\text{Var}(h_t|\theta)]}_{\text{Aleatoric Uncertainty}} + \underbrace{\text{Var}_\theta(\mathbb{E}[h_t|\theta])}_{\text{Epistemic Uncertainty}}. \quad (5)$$

Since in modern large language models, parameters are typically fixed at a point estimate, this variance decomposition relies on a Bayesian treatment of model parameters, such as deep ensembles, Monte Carlo dropout, or variational Inference. We build upon two common observations from prior work, noting that they are tendencies rather than absolute laws:

Peaked Parameter Posterior: In many well-trained LLMs, the parameters are often found in a region of a peaked posterior distribution $p(\theta|\mathcal{D})$ (Izmailov et al., 2018; Fort et al., 2019). This suggests that the parameter covariance $\Sigma_\theta = \text{Cov}(\theta)$ is often small, though not negligible, especially for under-regularized or smaller models.

Representational Expansion: Each transformer layer actively transforms and enriches its input, creating overcomplete representations in high dimensions (Sanford et al., 2023). This process inherently amplifies minor input variations, causing stochasticity to accumulate across layers (Schoenholz et al., 2016). However, this expansive potential is also constrained by key stabilizing mechanisms within the Transformer architecture, such as residual connections and layer normalization.

5.3 POTENTIAL DOMINANCE OF ALEATORIC UNCERTAINTY

The autoregressive process can be viewed as a Markov chain where sampling noise may accumulate through the network’s dynamics. We analyze the variance at step t for a fixed θ to gain intuition.

Lemma 1 (Variance Propagation with Expansion Property). *For a fixed parameter θ , the variance of the hidden state h_t can be bounded from below recursively. Assuming the transformation f exhibits representational expansion in deep Transformers (Wang et al., 2022; Schoenholz et al., 2016), the conditional variance satisfies:*

$$\mathbb{E}_\theta[\text{Var}(h_t|\theta)] \geq \mathbb{E}_\theta \mathbb{E}_{h_{t-1}} [|J_y(h_{t-1})|_F^2 \cdot \text{Var}(y_t|h_{t-1}; \theta)] + \Delta_{\text{nonlin}} \quad (6)$$

where $J_y = \frac{\partial f}{\partial y}$ is the Jacobian of the transformation with regard to the input token embedding, $|\cdot|_F$ denotes the Frobenius norm, and Δ_{nonlin} is a small term capturing higher-order effects.

Lemma 2 (Epistemic Uncertainty Bound). *The epistemic variance can be bounded by:*

$$\text{Var}_\theta(\mathbb{E}[h_t|\theta]) \leq \|G_t\|_F^2 \cdot \text{Tr}(\Sigma_\theta) + \epsilon_t \quad (7)$$

where $G_t = \frac{\partial \mathbb{E}[h_t|\theta]}{\partial \theta}$ is the sensitivity matrix of the expected hidden state trajectory to parameters, Σ_θ is the covariance of the parameter posterior, and ϵ_t is a non-linearity term in parameter space.

For detailed derivation and further discussion, please refer to Appendix C. Based on these lemmas, it is straightforward to obtain the final conclusion, noting its conditional nature.

Proposition 1. *For an autoregressive language model exhibiting a sufficiently peaked parameter posterior and representational expansion over t steps, the aleatoric uncertainty in its hidden representations may dominate the epistemic uncertainty:*

$$\mathbb{E}_\theta[\text{Var}(h_t|\theta)] \gg \text{Var}_\theta(\mathbb{E}[h_t|\theta]). \quad (8)$$

5.4 BRIDGING THEORY AND METHOD: THE NECESSITY OF A UNIFIED APPROACH

Our theoretical analysis underscores a critical challenge: the predominance of aleatoric uncertainty during a single forward pass without multiple samples obscures the epistemic uncertainty crucial for hallucination detection. With multiple samples, we can more easily probe the different paths the model considers, approaching the full picture of its internal probability distribution. This lets us externalize that distribution as semantic divergence, yielding richer and more visible uncertainty information for hallucination detection. However, this raises the question of how to best quantify this uncertainty. Relying solely on external metrics, such as the semantic entropy of final outputs,

discards the rich information within the model’s internal representations. Conversely, methods that focus purely on internal statistics, such as the Eigenscore which approximates the differential entropy of internal probability distribution, lack clear and interpretable associations with external semantic information. Meanwhile, our proposed method provides exactly such a unified view. By applying effective rank to hidden state embeddings collected from multiple sampled responses, it simultaneously (i) captures the “effective number of semantic categories” emerging externally across generations and (ii) encodes the dispersion of internal representations that reflect the probabilistic dynamics of the model.

In this way, Effective Rank-based Uncertainty bridges the gap between external semantic variation and internal interpretability. The effective rank method elegantly captures how the model’s internal representations continuously and interpretably transform into external semantic divergences. Therefore, we believe that further employing the effective rank method to study the external real-world meanings of internal representations is a highly promising direction.

6 CONCLUSION

In this work, we introduce the concept of Effective Rank-based Uncertainty, a spectral analysis tool, and apply it to the internal representations of LLMs, thereby proposing a simple and efficient method for hallucination detection. Through comprehensive experiments and ablation studies, we demonstrated the effectiveness of our approach. The practical interpretation of effective rank as the “effective number of distinct semantic categories in hidden representations” provides a clear and motivated basis for its application. Furthermore, by decomposing and quantitatively analyzing internal uncertainty, we provide in-depth theoretical modeling and analysis of the propagation of internal uncertainty noise in LLMs and how to leverage such uncertainty for hallucination detection. We believe that further exploration of effective rank as an elegant and powerful theoretical tool holds significant promise for enhancing the interpretability and reliability of AI systems.

ETHICS STATEMENT

Our overarching goal is to contribute to the development of safer AI systems by providing users with tools to better interpret the confidence and reliability of the output of the language model. In principle, such mechanisms could mitigate several risks associated with LLMs based on foundation models, including the production of misleading or harmful content in sensitive domains such as medicine. Nevertheless, this promise also carries potential downsides: systematic errors in uncertainty estimation, or poor communication of uncertainty, could foster misplaced trust and lead to unintended harms. Although our work advances methodological understanding and introduces new approaches for uncertainty quantification in LLM, we emphasize that deployment should be preceded by a careful, context-specific evaluation to ensure that the communicated uncertainty genuinely empowers users rather than creating confusion or false assurance.

REPRODUCIBILITY STATEMENT

Due to the high computational demands of experimentation with large foundation models, most prior work on uncertainty in LLM has depended on proprietary systems, costly fine-tuning procedures, or labor-intensive human evaluation, which can limit accessibility for many academic researchers. In contrast, our approach leverages recently released, openly available models and constructs a fully open-source pipeline for uncertainty quantification in LLM. Importantly, our method requires neither fine-tuning nor additional training of foundation models, and can be applied directly to pre-trained models in an “off-the-shelf” manner. We hope this design lowers barriers for future research in the academic community and facilitates straightforward replication of our experiments. Our open-source code is available at <https://github.com/1240148048/Effective-Rank-based-Uncertainty>.

REFERENCES

Yasin Abbasi Yadkori, Ilja Kuzborskij, András György, and Csaba Szepesvari. To believe or not to believe your llm: Iterative prompting for estimating epistemic uncertainty. *Advances in Neural Information Processing Systems*, 37:58077–58117, 2024.

Josh Achiam, Steven Adler, Sandhini Agarwal, Lama Ahmad, Ilge Akkaya, Florencia Leoni Aleman, Diogo Almeida, Janko Altenschmidt, Sam Altman, Shyamal Anadkat, et al. Gpt-4 technical report. *arXiv preprint arXiv:2303.08774*, 2023.

Gabriel Y Arteaga, Thomas B Schön, and Nicolas Pielawski. Hallucination detection in llms: Fast and memory-efficient fine-tuned models. *arXiv preprint arXiv:2409.02976*, 2024.

Chao Chen, Kai Liu, Ze Chen, Yi Gu, Yue Wu, Mingyuan Tao, Zhihang Fu, and Jieping Ye. Inside: Llms’ internal states retain the power of hallucination detection. *arXiv preprint arXiv:2402.03744*, 2024.

Stefan Depeweg, Jose-Miguel Hernandez-Lobato, Finale Doshi-Velez, and Steffen Udluft. Decomposition of uncertainty in bayesian deep learning for efficient and risk-sensitive learning. In *International conference on machine learning*, pp. 1184–1193. PMLR, 2018.

Sebastian Farquhar, Jannik Kossen, Lorenz Kuhn, and Yarin Gal. Detecting hallucinations in large language models using semantic entropy. *Nature*, 630(8017):625–630, 2024.

Angelos Filos, Sebastian Farquhar, Aidan N Gomez, Tim GJ Rudner, Zachary Kenton, Lewis Smith, Milad Alizadeh, Arnoud de Kroon, and Yarin Gal. Benchmarking bayesian deep learning with diabetic retinopathy diagnosis. *Preprint at https://arxiv.org/abs/1912.10481*, 2019.

Stanislav Fort, Huiyi Hu, and Balaji Lakshminarayanan. Deep ensembles: A loss landscape perspective. *arXiv preprint arXiv:1912.02757*, 2019.

Yarin Gal and Zoubin Ghahramani. Dropout as a bayesian approximation: Representing model uncertainty in deep learning. In *international conference on machine learning*, pp. 1050–1059. PMLR, 2016.

Baixiang Huang, Canyu Chen, Xiong Xiao Xu, Ali Payani, and Kai Shu. Can knowledge editing really correct hallucinations? *arXiv preprint arXiv:2410.16251*, 2024.

Lei Huang, Weijiang Yu, Weitao Ma, Weihong Zhong, Zhangyin Feng, Haotian Wang, Qianglong Chen, Weihua Peng, Xiaocheng Feng, Bing Qin, et al. A survey on hallucination in large language models: Principles, taxonomy, challenges, and open questions. *ACM Transactions on Information Systems*, 43(2):1–55, 2025.

Pavel Izmailov, Dmitrii Podoprikhin, Timur Garipov, Dmitry Vetrov, and Andrew Gordon Wilson. Averaging weights leads to wider optima and better generalization. *arXiv preprint arXiv:1803.05407*, 2018.

Albert Q. Jiang, Alexandre Sablayrolles, Arthur Mensch, Chris Bamford, Devendra Singh Chaplot, Diego de las Casas, Florian Bressand, Gianna Lengyel, Guillaume Lample, Lucile Saulnier, Lélio Renard Lavaud, Marie-Anne Lachaux, Pierre Stock, Teven Le Scao, Thibaut Lavril, Thomas Wang, Timothée Lacroix, and William El Sayed. Mistral 7b, 2023. URL <https://arxiv.org/abs/2310.06825>.

Mandar Joshi, Eunsol Choi, Daniel S Weld, and Luke Zettlemoyer. Triviaqa: A large scale distantly supervised challenge dataset for reading comprehension. *arXiv preprint arXiv:1705.03551*, 2017.

Saurav Kadavath, Tom Conerly, Amanda Askell, Tom Henighan, Dawn Drain, Ethan Perez, Nicholas Schiefer, Zac Hatfield-Dodds, Nova DasSarma, Eli Tran-Johnson, et al. Language models (mostly) know what they know. *arXiv preprint arXiv:2207.05221*, 2022.

Alex Kendall and Yarin Gal. What uncertainties do we need in bayesian deep learning for computer vision? *Advances in neural information processing systems*, 30, 2017.

Lorenz Kuhn, Yarin Gal, and Sebastian Farquhar. Semantic uncertainty: Linguistic invariances for uncertainty estimation in natural language generation. *arXiv preprint arXiv:2302.09664*, 2023.

Tom Kwiatkowski, Jennimaria Palomaki, Olivia Redfield, Michael Collins, Ankur Parikh, Chris Alberti, Danielle Epstein, Illia Polosukhin, Jacob Devlin, Kenton Lee, et al. Natural questions: a benchmark for question answering research. *Transactions of the Association for Computational Linguistics*, 7:453–466, 2019.

Balaji Lakshminarayanan, Alexander Pritzel, and Charles Blundell. Simple and scalable predictive uncertainty estimation using deep ensembles. *Advances in neural information processing systems*, 30, 2017.

Patrick Lewis, Ethan Perez, Aleksandra Piktus, Fabio Petroni, Vladimir Karpukhin, Naman Goyal, Heinrich Kütter, Mike Lewis, Wen-tau Yih, Tim Rocktäschel, et al. Retrieval-augmented generation for knowledge-intensive nlp tasks. *Advances in neural information processing systems*, 33: 9459–9474, 2020.

Chin-Yew Lin. Rouge: A package for automatic evaluation of summaries. In *Text summarization branches out*, pp. 74–81, 2004.

Andrey Malinin and Mark Gales. Uncertainty estimation in autoregressive structured prediction. *arXiv preprint arXiv:2002.07650*, 2020.

Potsawee Manakul, Adian Liusie, and Mark JF Gales. Selfcheckgpt: Zero-resource black-box hallucination detection for generative large language models. *arXiv preprint arXiv:2303.08896*, 2023.

Nay Myat Min, Long H Pham, Yige Li, and Jun Sun. Crow: Eliminating backdoors from large language models via internal consistency regularization. *arXiv preprint arXiv:2411.12768*, 2024.

Zachary Nado, Neil Band, Mark Collier, Josip Djolonga, Michael W Dusenberry, Sebastian Farquhar, Qixuan Feng, Angelos Filos, Marton Havasi, Rodolphe Jenatton, et al. Uncertainty baselines: Benchmarks for uncertainty & robustness in deep learning. *arXiv preprint arXiv:2106.04015*, 2021.

Pranav Rajpurkar, Jian Zhang, Konstantin Lopyrev, and Percy Liang. Squad: 100,000+ questions for machine comprehension of text. *arXiv preprint arXiv:1606.05250*, 2016.

Olivier Roy and Martin Vetterli. The effective rank: A measure of effective dimensionality. In *2007 15th European signal processing conference*, pp. 606–610. IEEE, 2007.

Clayton Sanford, Daniel J Hsu, and Matus Telgarsky. Representational strengths and limitations of transformers. *Advances in Neural Information Processing Systems*, 36:36677–36707, 2023.

Samuel S Schoenholz, Justin Gilmer, Surya Ganguli, and Jascha Sohl-Dickstein. Deep information propagation. *arXiv preprint arXiv:1611.01232*, 2016.

Oscar Skean, Md Rifat Arefin, Dan Zhao, Niket Patel, Jalal Naghiyev, Yann LeCun, and Ravid Shwartz-Ziv. Layer by layer: Uncovering hidden representations in language models. *arXiv preprint arXiv:2502.02013*, 2025.

Gemini Team, Rohan Anil, Sebastian Borgeaud, Jean-Baptiste Alayrac, Jiahui Yu, Radu Soricu, Johan Schalkwyk, Andrew M Dai, Anja Hauth, Katie Millican, et al. Gemini: a family of highly capable multimodal models. *arXiv preprint arXiv:2312.11805*, 2023.

SMTI Tonmoy, SM Zaman, Vinija Jain, Anku Rani, Vipula Rawte, Aman Chadha, and Amitava Das. A comprehensive survey of hallucination mitigation techniques in large language models. *arXiv preprint arXiv:2401.01313*, 6, 2024.

Hugo Touvron, Louis Martin, Kevin Stone, Peter Albert, Amjad Almahairi, Yasmine Babaei, Nikolay Bashlykov, Soumya Batra, Prajjwal Bhargava, Shruti Bhosale, et al. Llama 2: Open foundation and fine-tuned chat models. *arXiv preprint arXiv:2307.09288*, 2023.

George Tsatsaronis, Georgios Balikas, Prodromos Malakasiotis, Ioannis Partalas, Matthias Zschunke, Michael R Alvers, Dirk Weissenborn, Anastasia Krithara, Sergios Petridis, Dimitris Polychronopoulos, et al. An overview of the bioasq large-scale biomedical semantic indexing and question answering competition. *BMC bioinformatics*, 16(1):138, 2015.

Peihao Wang, Wenqing Zheng, Tianlong Chen, and Zhangyang Wang. Anti-oversmoothing in deep vision transformers via the fourier domain analysis: From theory to practice. *arXiv preprint arXiv:2203.05962*, 2022.

Fanghua Ye, Mingming Yang, Jianhui Pang, Longyue Wang, Derek Wong, Emine Yilmaz, Shuming Shi, and Zhaopeng Tu. Benchmarking llms via uncertainty quantification. *Advances in Neural Information Processing Systems*, 37:15356–15385, 2024.

Yuji Zhang, Sha Li, Cheng Qian, Jiateng Liu, Pengfei Yu, Chi Han, Yi R Fung, Kathleen McKeown, Chengxiang Zhai, Manling Li, et al. The law of knowledge overshadowing: Towards understanding, predicting, and preventing llm hallucination. *arXiv preprint arXiv:2502.16143*, 2025.

Zhijian Zhuo, Yifei Wang, Jinwen Ma, and Yisen Wang. Towards a unified theoretical understanding of non-contrastive learning via rank differential mechanism. *arXiv preprint arXiv:2303.02387*, 2023.

A THE USE OF LARGE LANGUAGE MODELS (LLMs)

In preparing this manuscript, we made limited use of LLMs solely to aid in polishing the writing. Specifically, LLMs were used for improving grammar, clarity, and style of exposition. All conceptual development, technical contributions, theoretical results, and experimental analyses were conceived and carried out entirely by the authors. The scientific content, data analysis, and conclusions remain exclusively the responsibility of the authors.

B MORE THEORETICAL BACKGROUND ON EFFECTIVE RANK

A key theoretical perspective motivating our approach comes from the information-theoretic interpretation of Shannon entropy. Given a categorical distribution $p = (p_1, p_2, \dots, p_C)$, the Shannon entropy is defined as $H(p) = -\sum_{i=1}^C p_i \log p_i$. While H is commonly viewed as a measure of uncertainty, it also directly encodes the notion of an effective number of categories, defined as $N_{\text{eff}}(p) = \exp(H(p))$. This quantity represents the number of outcomes in a uniform distribution that would yield the same level of uncertainty as p . For instance,

$$p = [0.8, 0.1, 0.1] \Rightarrow H(p) \approx 0.639, \quad N_{\text{eff}} \approx 1.89,$$

whereas

$$p = [0.3, 0.3, 0.4] \Rightarrow H(p) \approx 1.089, \quad N_{\text{eff}} \approx 2.97.$$

Although both are distributions over three categories, the first case exhibits a stronger bias towards a single outcome, hence the small probabilities 0.1 are more likely to represent noise or modeling errors rather than genuine equiprobable alternatives, whereas the second distribution is closer to true ambiguity among three plausible options. This principle is precisely the motivation behind the notion of effective rank, introduced in (Roy & Vetterli, 2007). Analogous to the effective number of categories, effective rank measures the *effective dimensionality* of the matrix, which in our method corresponds to the number of equivalent semantic categories represented by the embedding vectors. As shown in Figure 2, we can intuitively see how the effective rank continuously measures the degree of divergence of matrix vectors.

Moreover, the effective rank employs the singular value distribution to calculate the Shannon entropy because the singular values of a matrix inherently capture information about the direction and magnitude distribution of its internal vectors. The more uniform the singular value distribution, the more dispersed the linearly independent vector groups within the matrix are; conversely, the more concentrated they are:

- If all column vectors share the same direction, then A has rank one, and there is only a single non-zero singular value, thus $H = 0$, $\exp(H) = 1$, implying complete certainty.
- If all column vectors have the same length and are pairwise orthogonal, then all singular values are equal. In this case, $H = -\sum_{i=1}^m \frac{1}{m} \ln(\frac{1}{m}) = \ln m$, $\exp(H) = m$, which corresponds to maximal uncertainty.

We prove that the effective rank of a matrix is always less than or equal to its true rank, and the equality holds if and only if the two conditions above are satisfied. Let A be a matrix with singular values $\sigma_1, \sigma_2, \dots, \sigma_n$ where n is the minimum dimension of A . The normalized singular values are defined as $p_i = \sigma_i / \|\sigma\|_1$, where $\|\sigma\|_1 = \sum_{i=1}^n \sigma_i$. The entropy of A is given by $H(A) = -\sum_{i=1}^n p_i \log p_i$ (with $0 \log 0 = 0$), and the entropy-based effective rank is $\text{erank}(A) = \exp(H(A))$. The true rank is $r = \text{rank}(A)$, the number of non-zero singular values.

To prove $\text{erank}(A) \leq r$, we apply Jensen's inequality to the concave function $\log x$:

$$H(A) = \sum_{i:p_i > 0} p_i \log \left(\frac{1}{p_i} \right) \leq \log \left(\sum_{i:p_i > 0} p_i \cdot \frac{1}{p_i} \right) = \log r \quad (9)$$

where the sum is over the r indices with $p_i > 0$. Thus, $\text{erank}(A) = \exp(H(A)) \leq \exp(\log r) = r$.

Equality holds if and only if all non-zero singular values are equal, since $\log x$ is strictly concave and equality in Jensen's inequality requires that all $1/p_i$ are equal for $p_i > 0$, meaning $p_i = 1/r$ for each non-zero singular value.

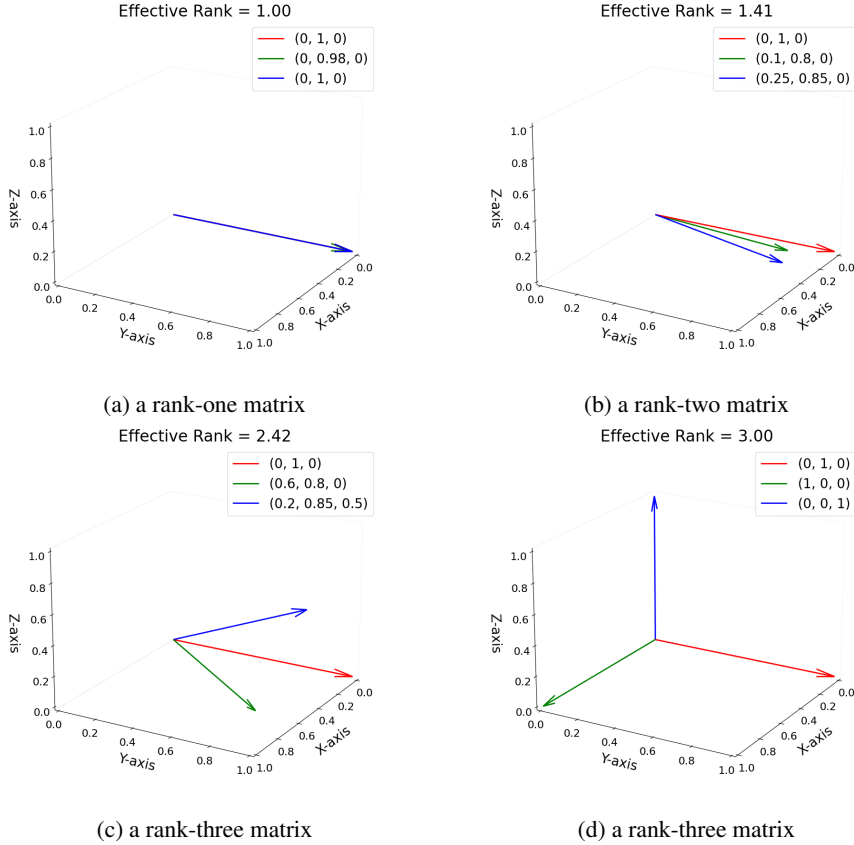


Figure 2: Visualization of Effective Ranks

C PROOFS AND DISCUSSION

This appendix provides the detailed proofs for the lemmas and proposition stated in the main text.

C.1 PROOF OF LEMMA 1

(Variance Propagation with Expansion Property) For a fixed parameter θ , the variance of the hidden state h_t can be bounded from below recursively. Assuming the transformation f exhibits representational expansion in deep Transformers, the conditional variance satisfies:

$$\mathbb{E}_\theta[\text{Var}(h_t|\theta)] \geq \mathbb{E}_\theta \mathbb{E}_{h_{t-1}} [|J_y(h_{t-1})|_F^2 \cdot \text{Var}(y_t|h_{t-1}; \theta)] + \Delta_{\text{nonlin}} \quad (10)$$

where $J_y = \frac{\partial f}{\partial y}$ is the Jacobian of the transformation with regard to the input token embedding, $|\cdot|_F$ denotes the Frobenius norm, and Δ_{nonlin} is a non-negative term capturing higher-order effects that typically amplify variance.

Proof. We analyze the evolution of the variance through the deterministic function $h_t = f(h_{t-1}, y_t; \theta)$. Our goal is to find a lower bound for $\text{Var}(h_t|\theta)$.

We begin by applying the law of total variance conditional on θ :

$$\text{Var}(h_t|\theta) = \mathbb{E}_{h_{t-1}}[\text{Var}(h_t|h_{t-1}, \theta)] + \text{Var}_{h_{t-1}}(\mathbb{E}[h_t|h_{t-1}, \theta]) \quad (11)$$

We now analyze each term separately.

1. Analysis of $\mathbb{E}_{h_{t-1}}[\text{Var}(h_t|h_{t-1}, \theta)]$:

Given h_{t-1} , the randomness in h_t comes solely from y_t . Let us define the conditional mean of the next token:

$$\mu_y(h_{t-1}) = \mathbb{E}[y_t|h_{t-1}; \theta]$$

We perform a first-order Taylor expansion of the function f around the point $(h_{t-1}, \mu_y(h_{t-1}))$:

$$h_t = f(h_{t-1}, y_t; \theta) = f(h_{t-1}, \mu_y; \theta) + J_y(h_{t-1}) \cdot (y_t - \mu_y) + R(h_{t-1}, y_t) \quad (12)$$

where $J_y(h_{t-1}) = \frac{\partial f(h_{t-1}, y; \theta)}{\partial y} \Big|_{y=\mu_y}$ is the Jacobian matrix, $R(h_{t-1}, y_t)$ is the Taylor remainder term, which encapsulates all higher-order derivatives.

Taking the conditional expectation $\mathbb{E}[\cdot|h_{t-1}, \theta]$ of Eq. 12:

$$\begin{aligned} \mathbb{E}[h_t|h_{t-1}, \theta] &= f(h_{t-1}, \mu_y; \theta) + J_y(h_{t-1}) \cdot \underbrace{\mathbb{E}[(y_t - \mu_y)|h_{t-1}, \theta]}_{=0} + \mathbb{E}[R|h_{t-1}, \theta] \\ &= f(h_{t-1}, \mu_y; \theta) + \mathbb{E}[R|h_{t-1}, \theta] \end{aligned}$$

The conditional variance $\text{Var}(h_t|h_{t-1}, \theta)$ is the variance of the right-hand side of Eq. 12 around this conditional mean. Neglecting the covariance between the linear and remainder terms, we can approximate:

$$\text{Var}(h_t|h_{t-1}, \theta) \gtrsim \text{Var}(J_y(h_{t-1})(y_t - \mu_y) | h_{t-1}, \theta) + \text{Var}(R|h_{t-1}, \theta) \quad (13)$$

The first term is the variance of the linear approximation. Assuming J_y is approximately constant over the variation of y_t (because the internal transformations of well-trained LLMs often exhibit a certain degree of consistency in generating different sequences), this variance can be expressed as:

$$\text{Var}(J_y(y_t - \mu_y) | h_{t-1}, \theta) = J_y \cdot \text{Var}(y_t|h_{t-1}; \theta) \cdot J_y^\top$$

The total variance of this linear term is the trace of this covariance matrix:

$$\text{Tr}(J_y \cdot \text{Var}(y_t|h_{t-1}; \theta) \cdot J_y^\top) = \text{Tr}(J_y^\top J_y \cdot \text{Var}(y_t|h_{t-1}; \theta)) = |J_y|_F^2 \cdot \text{Var}(y_t|h_{t-1}; \theta)$$

The second term in Eq. 13, $\text{Var}(R|h_{t-1}, \theta)$, is the variance of the remainder. For common modern activation functions which are smooth and exhibit local linearity, and under the influence of layer normalization which constrains inputs, the remainder term R is typically small. We denote this small contribution as $\delta_{\text{nonlin}}(h_{t-1})$. Crucially, for expansive transformations (Sanford et al., 2023; Wang et al., 2022), the higher-order terms often amplify variance rather than suppress it. Moreover, J_y itself contains a large amount of parameter information. Therefore, the Frobenius norm $|J_y(h_{t-1})|_F$, which represents the square root of the sum of the squares of the matrix elements, is often much greater than 1.

Thus, we can write:

$$\text{Var}(h_t|h_{t-1}, \theta) \gtrsim |J_y(h_{t-1})|_F^2 \cdot \text{Var}(y_t|h_{t-1}; \theta) + \delta_{\text{nonlin}}(h_{t-1}) \quad (14)$$

Taking the expectation of Eq. 14 with respect to h_{t-1} and θ gives the first term of our final bound:

$$\mathbb{E}_\theta \mathbb{E}_{h_{t-1}} [\text{Var}(h_t|h_{t-1}, \theta)] \geq \mathbb{E}_\theta \mathbb{E}_{h_{t-1}} [|J_y(h_{t-1})|_F^2 \cdot \text{Var}(y_t|h_{t-1}; \theta)] + \Delta_{\text{nonlin}}^{(1)} \quad (15)$$

where $\Delta_{\text{nonlin}}^{(1)} = \mathbb{E}_\theta \mathbb{E}_{h_{t-1}} [\delta_{\text{nonlin}}(h_{t-1})]$. \square

C.2 PROOF OF LEMMA 2

[Epistemic Uncertainty Bound] The epistemic variance can be bounded by:

$$\text{Var}_\theta(\mathbb{E}[h_t|\theta]) \leq |G_t|_F^2 \cdot \text{Tr}(\Sigma\theta) + \epsilon_t$$

Proof. Let $\mu_\theta = \mathbb{E}[\theta]$ be the mean of the parameter posterior distribution and $\delta = \theta - \mu_\theta$ be the zero-mean perturbation vector with covariance $\Sigma_\theta = \mathbb{E}[\delta\delta^\top]$.

Consider the expected hidden state $\mu_h(\theta) = \mathbb{E}[h_t|\theta]$ as a function of the parameters. We perform a first-order Taylor expansion around μ_θ :

$$\mu_h(\theta) = \mu_h(\mu_\theta + \delta) \approx \mu_h(\mu_\theta) + G_t \cdot \delta \quad (16)$$

where $G_t = \frac{\partial \mu_h(\theta)}{\partial \theta} \bigg|_{\theta=\mu\theta}$, G_t is the Jacobian matrix describing the sensitivity of the expected hidden state to parameter changes. The variance of $\mu_h(\theta)$ is then:

$$\text{Var}_\theta(\mathbb{E}[h_t|\theta]) = \text{Var}_\theta(\mu_h(\theta)) \approx \text{Var}_\theta(G_t \cdot \delta) = \mathbb{E}[(G_t \delta)(G_t \delta)^\top] = G_t \mathbb{E}[\delta \delta^\top] G_t^\top = G_t \Sigma_\theta G_t^\top \quad (17)$$

To find the total variance, we take the trace of this covariance matrix:

$$\text{Tr}(\text{Var}_\theta(\mu_h(\theta))) \approx \text{Tr}(G_t \Sigma_\theta G_t^\top) = \text{Tr}(G_t^\top G_t \Sigma_\theta) \quad (18)$$

Applying the Cauchy-Schwarz inequality for the trace (von Neumann's trace inequality), we get:

$$\text{Tr}(G_t^\top G_t \Sigma_\theta) \leq \sqrt{\text{Tr}((G_t^\top G_t)^2) \cdot \text{Tr}(\Sigma_\theta^2)} \quad (\text{a}) \leq \text{Tr}(G_t^\top G_t) \cdot \text{Tr}(\Sigma_\theta) \quad (\text{b}) \quad (19)$$

Inequality (a) is the Cauchy-Schwarz application. Inequality (b) holds because: $\text{Tr}(A^2) \leq (\text{Tr}(A))^2$ for a positive semidefinite matrix A . Noting that $\text{Tr}(G_t^\top G_t) = |G_t|_F^2$, we arrive at:

$$\text{Tr}(\text{Var}_\theta(\mu_h(\theta))) \lesssim |G_t|_F^2 \cdot \text{Tr}(\Sigma_\theta)$$

The term ϵ_t is introduced to account for the error in the first-order Taylor approximation, which includes the effects of higher-order derivatives. This error is typically small if the function $\mu_h(\theta)$ is approximately linear in θ in the region of high posterior probability, an assumption linked to a peaked posterior. \square

C.3 PROOF OF PROPOSITION 1

For an autoregressive language model exhibiting a sufficiently peaked parameter posterior and representational expansion over t steps, the aleatoric uncertainty in its hidden representations may dominate the epistemic uncertainty:

$$\mathbb{E}_\theta[\text{Var}(h_t|\theta)] \gg \text{Var}_\theta(\mathbb{E}[h_t|\theta]) \quad (20)$$

Proof. Let $a_t = \mathbb{E}_\theta[\text{Var}(h_t|\theta)]$ (aleatoric) and $e_t = \text{Var}_\theta(\mathbb{E}[h_t|\theta])$ (epistemic).

From Lemma 1, the aleatoric term follows a recursive inequality:

$$a_t \gtrsim \mathbb{E}_\theta \mathbb{E}_{h_{t-1}} [|J_y(h_{t-1})|_F^2 \cdot \text{Var}(y_t|h_{t-1}; \theta)]$$

Under the *representational expansion* assumption, the expected Jacobian norm $\mathbb{E}[|J_y|_F^2]$ is large ($\gg 1$). Furthermore, for most tokens in a generation, the predictive distribution $p(y_t|h_{t-1}; \theta)$ has high entropy, meaning $\text{Var}(y_t|h_{t-1}; \theta)$ is also significant. The product of these two large factors is a large positive quantity at each step t .

From Lemma 2, the epistemic term is bounded:

$$e_t \leq |G_t|_F^2 \cdot \text{Tr}(\Sigma_\theta) + \epsilon_t$$

Under the *peaked parameter posterior* assumption, $\text{Tr}(\Sigma_\theta)$ is small. The sensitivity $|G_t|_F^2$ of the expected hidden state to parameters depends on the model's stability. In a well-trained robust transformer with residual connections and layer normalization, the expected representations are often stable with respect to small parameter perturbations, restricting $|G_t|_F^2$ to a smaller range. The error term ϵ_t from the linear approximation is also small due to the peaked posterior. Consequently, e_t remains bounded by a relatively small constant as t increases.

Therefore, for each step t , the recursive accumulation of sampling noise through expansive transformations causes a_t to become much larger than the bounded epistemic term e_t , leading to the stated dominance: $a_t \gg e_t$. \square

C.4 DISCUSSION OF LIMITATIONS

It is important to emphasize that the above analysis is heuristic rather than a strict universal proof. Several limitations apply. First, the variance decomposition in Eq. 5 is borrowed from Bayesian

deep learning for model outputs, but here it is applied to hidden states of autoregressive LLMs. This approach is heuristic and requires us to define the distribution function of LLM parameters in additional ways (although in practical applications, the parameters of LLMs are often given). Second, Lemma 1 relies on first-order Taylor expansions; the neglected higher-order term Δ_{nonlin} may be non-negligible in some cases. Finally, the bound on epistemic uncertainty in Lemma 2 assumes a concentrated posterior distribution and smooth sensitivity to parameters. While reasonable for large pretrained models, this may not hold for small or under-regularized ones. Therefore, the dominance of aleatoric over epistemic uncertainty in Proposition 1 should be viewed as a qualitative tendency under certain conditions, not a universal law. We highlight these caveats to clarify that our theoretical motivation is primarily heuristic, aiming to explain why single-pass-based hallucination is often unreliable and provide interpretable insights for future works.

D ADDITIONAL EXPERIMENTAL DATA

Here are the complete data from our ablation study on the number of generations, hidden-layer selection strategy, and temperature. It offers a finer-grained view of how the information encoded in hidden-layer representations interacts with these hyper-parameters.

N	Dataset	M1	M5	L1	L5	ES	PF	DSE	LNE	SE
10	TriviaQA	0.7877	0.7700	0.7809	0.7629	0.7802	0.6625	0.7758	0.6947	0.7750
	SQuAD	0.7212	0.7217	0.7191	0.7190	0.7199	0.6594	0.7172	0.6505	0.7181
	BioASQ	0.8447	0.8461	0.8481	0.8472	0.8433	0.7321	0.8437	0.4703	0.8425
	NQ	0.7029	0.7038	0.7036	0.7049	0.7056	0.6584	0.6984	0.6495	0.7001
Average		0.7641	0.7604	0.7629	0.7585	0.7623	0.6781	0.7588	0.6163	0.7589
15	TriviaQA	0.7862	0.7902	0.787	0.7807	0.7825	0.6579	0.7813	0.7211	0.7768
	SQuAD	0.7407	0.7407	0.7391	0.7395	0.7391	0.7148	0.7349	0.6070	0.7381
	BioASQ	0.8715	0.8690	0.8684	0.8678	0.8682	0.7496	0.8648	0.4748	0.8615
	NQ	0.7182	0.7166	0.7174	0.7188	0.7206	0.6598	0.7148	0.6823	0.7157
Average		0.7792	0.7791	0.7780	0.7767	0.7776	0.6955	0.7740	0.6213	0.7730
20	TriviaQA	0.7786	0.7780	0.7729	0.7702	0.7743	0.6636	0.7671	0.7180	0.7698
	SQuAD	0.7596	0.7604	0.7599	0.7610	0.7579	0.6791	0.7588	0.6583	0.7581
	BioASQ	0.8645	0.8625	0.8638	0.8620	0.8628	0.7517	0.8564	0.4570	0.8585
	NQ	0.7277	0.7292	0.7274	0.7278	0.7284	0.6551	0.7243	0.6599	0.7256
Average		0.7826	0.7825	0.7810	0.7803	0.7809	0.6874	0.7767	0.6233	0.7780

Table 5: Ablation studies on Llama-2-7b-chat, where N refers to the number of generations, M1 refers to extracting the exact middle hidden layer for each answer in the ER method, M5 refers to extracting the middle five layers, L1 refers to extracting the last layer, and L5 refers to extracting the last five layers, ES denotes Eigenscore, PF denotes P_False, DSE denotes Discrete Semantic Entropy, LNE denotes Length-Normalized Entropy, and SE denotes Semantic Entropy. All numbers in the table are AUROC scores; values closer to 1 indicate stronger hallucination-detection ability

E CASE STUDY

Below, we provide several specific examples from the main experiment. Please refer to Appendix F for the discussion.

N	Dataset	M1	M5	L1	L5	ES	PF	DSE	LNE	SE
10	TriviaQA	0.7407	0.7516	0.7302	0.7495	0.7342	0.7379	0.7331	0.6930	0.7390
	SQuAD	0.7259	0.7273	0.7241	0.7228	0.7239	0.6945	0.7381	0.6886	0.7350
	BioASQ	0.8234	0.8277	0.8318	0.8324	0.8215	0.7980	0.7951	0.5610	0.7988
	NQ	0.7284	0.7290	0.7286	0.7352	0.7270	0.6841	0.7234	0.6866	0.7258
Average		0.7546	0.7589	0.7537	0.7600	0.7517	0.7286	0.7474	0.6573	0.7497
15	TriviaQA	0.7763	0.7672	0.7681	0.7781	0.7654	0.7249	0.7590	0.6446	0.7577
	SQuAD	0.7289	0.7289	0.7271	0.7285	0.7264	0.6747	0.7393	0.6823	0.7379
	BioASQ	0.8358	0.8313	0.8341	0.8313	0.8328	0.7490	0.8224	0.4874	0.8148
	NQ	0.7015	0.6996	0.7045	0.7054	0.7038	0.6902	0.6999	0.6452	0.6936
Average		0.7606	0.7560	0.7577	0.7601	0.7571	0.7097	0.7567	0.6149	0.7523
20	TriviaQA	0.7439	0.7553	0.7446	0.7339	0.7246	0.7294	0.7413	0.6953	0.7429
	SQuAD	0.7331	0.7306	0.7293	0.7291	0.7299	0.6589	0.7382	0.6874	0.7360
	BioASQ	0.8409	0.8454	0.8411	0.8461	0.8413	0.7864	0.8279	0.5939	0.8299
	NQ	0.7178	0.7155	0.7193	0.7185	0.7175	0.6428	0.7149	0.6880	0.7120
Average		0.7589	0.7617	0.7586	0.7569	0.7533	0.7044	0.7556	0.6662	0.7552

Table 6: Ablation studies on Llama-2-13b-chat about the number of generations and hidden layer vector extraction strategy

N	Dataset	M1	M5	L1	L5	ES	PF	DSE	LNE	SE
10	TriviaQA	0.7634	0.7650	0.7651	0.7637	0.7579	0.7239	0.7575	0.6519	0.7553
	SQuAD	0.7208	0.7144	0.7073	0.7080	0.7120	0.6333	0.7227	0.6223	0.7238
	BioASQ	0.8563	0.8584	0.8506	0.8475	0.8513	0.7173	0.8507	0.5955	0.8513
	NQ	0.7658	0.7696	0.7614	0.7611	0.7627	0.7523	0.7678	0.6770	0.7662
Average		0.7766	0.7769	0.7711	0.7701	0.7710	0.7067	0.7747	0.6367	0.7742
15	TriviaQA	0.7727	0.7767	0.7727	0.7720	0.7706	0.7265	0.7660	0.7058	0.7676
	SQuAD	0.6952	0.7064	0.6936	0.6907	0.6866	0.6047	0.7041	0.6529	0.6991
	BioASQ	0.8586	0.8548	0.8539	0.8557	0.8557	0.6866	0.8551	0.6129	0.8560
	NQ	0.7859	0.7861	0.7886	0.7896	0.7826	0.7717	0.7826	0.6975	0.7828
Average		0.7781	0.7810	0.7772	0.7770	0.7739	0.6974	0.7770	0.6673	0.7764
20	TriviaQA	0.7677	0.7672	0.7599	0.7688	0.7644	0.7663	0.7569	0.6861	0.7623
	SQuAD	0.7433	0.7480	0.7413	0.7384	0.7371	0.5995	0.7559	0.6782	0.7533
	BioASQ	0.8670	0.8662	0.8630	0.8631	0.8641	0.7594	0.8617	0.5854	0.8645
	NQ	0.7754	0.7749	0.7723	0.7724	0.7695	0.7709	0.7736	0.7046	0.7712
Average		0.7884	0.7891	0.7841	0.7857	0.7838	0.7240	0.7870	0.6636	0.7878

Table 7: Ablation studies on Mistral-7B-v0.1 about the number of generations and hidden layer vector extraction strategy

E.1 TRIVIAQA DATASET ON LLAMA-2-7B-CHAT

Question: Who was the first man sent into space, in 1961?

Correct Answer: ['gagarin']

LLM's Answer: yuri gagarin

Accuracy: 1.0

Sampled Responses: ['yuri gagarin', 'yuri gagarin']

Singular Values: [76.35235595703125, 2.6761877219491637e-14, 1.1108339471383637e-15, 2.146262724714404e-30, 3.9155441760212304e-31, 0.0, 0.0, 0.0, 0.0, 0.0]

Effective Rank: 1.0000000000000002

Eigenscore: -61.72965268471336

t	Dataset	M1	M5	L1	L5	ES	PF	DSE	LNE	SE
0.1	TriviaQA	0.6514	0.6660	0.6782	0.6503	0.6200	0.6695	0.6263	0.5391	0.6466
	SQuAD	0.6451	0.6466	0.6118	0.5971	0.6038	0.6413	0.6125	0.5506	0.6333
	BioASQ	0.7336	0.6834	0.7268	0.7416	0.6923	0.7720	0.7085	0.4401	0.7352
	NQ	0.6771	0.6665	0.6841	0.6664	0.6673	0.7308	0.6700	0.6231	0.6822
Average		0.6768	0.6656	0.6752	0.6639	0.6459	0.7034	0.6543	0.5382	0.6743
0.5	TriviaQA	0.7438	0.7628	0.7518	0.7492	0.7350	0.6806	0.7280	0.5880	0.7154
	SQuAD	0.7364	0.7391	0.7392	0.7401	0.7330	0.6551	0.7308	0.6104	0.7318
	BioASQ	0.8432	0.8374	0.8449	0.8452	0.8378	0.7320	0.8355	0.5167	0.8293
	NQ	0.7679	0.7671	0.7724	0.7678	0.7641	0.7516	0.7643	0.6356	0.7629
Average		0.7728	0.7766	0.7771	0.7756	0.7675	0.7048	0.7647	0.5877	0.7599
1.0	TriviaQA	0.7634	0.7650	0.7651	0.7637	0.7579	0.7239	0.7575	0.6519	0.7553
	SQuAD	0.7208	0.7144	0.7073	0.7080	0.7120	0.6333	0.7227	0.6223	0.7238
	BioASQ	0.8563	0.8584	0.8506	0.8475	0.8513	0.7173	0.8507	0.5955	0.8513
	NQ	0.7658	0.7696	0.7614	0.7611	0.7627	0.7523	0.7678	0.6770	0.7662
Average		0.7766	0.7769	0.7711	0.7701	0.7710	0.7067	0.7747	0.6367	0.7742
2.0	TriviaQA	0.6679	0.6685	0.6651	0.6662	0.6545	0.7084	0.6643	0.6234	0.6666
	SQuAD	0.5754	0.5502	0.5593	0.5407	0.5698	0.5603	0.5213	0.5633	0.5592
	BioASQ	0.7280	0.7329	0.7106	0.7238	0.6998	0.6867	0.7243	0.5534	0.7244
	NQ	0.6034	0.6031	0.6118	0.6069	0.5788	0.7006	0.5996	0.5580	0.5906
Average		0.6437	0.6387	0.6367	0.6344	0.6257	0.6640	0.6274	0.5745	0.6352

Table 8: Ablation studies on Mistral-7B-v0.1 about temperature, where t denotes temperature

Question: September 9, 1969 saw what made an official language of Canada?

Correct Answer: ['french']

LLM's Answer: french

Accuracy: 1.0

Sampled Responses: ['Quebec', 'french', 'french', 'Quebec', 'constitution', 'Quebec', 'french', 'french', 'french']

Singular Values: [60.25969314575195, 41.63536071777344, 24.346080780029297, 1.6957731741170864e-14, 5.443248018391789e-15, 1.19803634661477e-15, 8.686304874642721e-16, 1.4343240353264575e-16, 8.151879937535818e-32, 2.8225723498131095e-32]

Effective Rank: 2.818618681563689

Eigenscore: -51.25870849393463

Question: In which part of the human body would you find the Sphenoid bone?

Correct Answer: ['skull']

LLM's Answer: brain

Accuracy: 0.0

Sampled Responses: ['head', 'brain', 'skull', 'skull', 'skull', 'head', 'brain', 'skull', 'skull']

Singular Values: [58.72682571411133, 34.81084442138672, 29.228200912475586, 7.700909307212667e-15, 7.15308397231237e-15, 2.269143032179147e-15, 3.835939579384829e-16, 3.338613852606579e-30, 1.4536969531393071e-31, 7.850294372204882e-33]

Effective Rank: 2.8627889069115606

Eigenscore: -51.30254888163167

E.2 SQuAD DATASET ON MISTRAL-7B-v0.1

Question: Who did Frick remove from the police force?

Correct Answer: ['anyone he suspected of being a republican']

LLM's Answer: the corrupt

Accuracy: 0.0

Sampled Responses: ['the corrupt', 'the corrupt']

Singular Values: [1139.242431640625, 3.5298562575496184e-13, 1.458547028271827e-14, 3.75700543160097e-29, 3.410722249588845e-30, 2.802596928649634e-45, 1.401298464324817e-45, 0.0, 0.0, 0.0]

Effective Rank: 1.0000000000000004

Eigenscore: -64.89193565768241

Question: Who verbally attacked Steve Stone?

Correct Answer: ['Kent Mercker']

LLM's Answer: Steve Stone

Accuracy: 0.0

Sampled Responses: ['Joe Morgan', 'his boss', 'John Kruk', 'Steve Stone', 'Steve Stone', 'his boss', 'John Madden', 'his boss', 'his boss']

Singular Values: [1180.1435546875, 552.9315185546875, 154.78468322753906, 16.52665138244629, 6.953697204589844, 1.193859735463404e-13, 1.553780128377754e-14, 6.809435505831249e-16, 1.553959034971104e-17, 1.1361135973578757e-30]

Effective Rank: 2.513272471125542

Eigenscore: -61.32968780733988

Question: In 2002 what act granted full British citizenship to the citizens of the islands?

Correct Answer: ['British Overseas Territories Act 2002']

LLM's Answer: British Overseas Territories Act

Accuracy: 1.0

Sampled Responses: ['British Overseas Territories Act', 'British Nationality Act', 'British Overseas Territories Act', 'British Overseas Territories Act', 'British Overseas Territories Act']

Singular Values: [1153.8829345703125, 328.6450500488281, 7.30688702902868e-14, 2.118430780068855e-30, 1.2843073833195104e-33, 0.0, 0.0, 0.0, 0.0, 0.0]

Effective Rank: 1.6972759552279857

Eigenscore: -63.12688798174471

E.3 BIOASQ DATASET ON LLAMA-2-13B-CHAT

Question: Which are the thyroid hormone analogs utilized in human studies?

Correct Answer: ['TRIAC']

LLM's Answer: Liothyronine (T3) and levothyroxine (T4)

Accuracy: 0.0

Sampled Responses: ['triiodothyronine (T3) and levothyroxine (T4)', 'Liothyronine and levothyroxine', 'Liothyronine (T3) and levothyroxine (T4)', 'liothyronine and levothyroxine']

Singular Values: [218.68751525878906, 62.00069046020508, 15.469388961791992, 3.4699248902941024e-15, 3.3113897569630145e-15, 4.50245604514668e-31, 1.978491468987644e-31, 2.0052295279776766e-32, 0.0, 0.0]

Effective Rank: 2.0248367530554368

Eigenscore: -53.52278438073435

Question: Which genes are involved in patient response to warfarin?

Correct Answer: ['CYP2C9', 'VKORC1', 'ORM1', 'CYP4F2', 'EPHX1', 'CYP2C18', 'CYP2C19', 'CYP3A5', 'protein S', 'clotting factor V', 'PROC', 'GGCX']

LLM's Answer: VKORC1 and CYP2C9

Accuracy: 1.0

Sampled Responses: ['VKORC1 and CYP2C9', 'VKORC1 and CYP2C9', 'CYP2C9 and VKORC1', 'VKORC1 and CYP2C9', 'CYP2C9, VKORC1, and CYP3A4', 'CYP2C9, VKORC1, and CYP3A4', 'VKORC1 and CYP2C9', 'VKORC1 and CYP2C9', 'CYP2C9 and VKORC1']

Singular Values: [217.03753662109375, 100.93067932128906, 6.290593147277832, 4.6974177206424855e-15, 2.6008424048733518e-15, 1.8994920306458578e-16, 1.1646331124343226e-16, 8.127036452178364e-32, 1.1876486869033015e-33, 0.0]

Effective Rank: 2.0309090152250144

Eigenscore: -53.3001540843245

Question: List symptoms of the IFAP syndrome.

Correct Answer: ['follicular ichthyosis', 'atrichia', 'photophobia']

LLM's Answer: intellectual disability, fibrosis, alopecia, and pigmentary changes.

Accuracy: 0.0

Sampled Responses: ['ichthyosis, facial dysmorphism, arthrogryposis, and pul', 'intellectual disability, fibrosis, alopecia, and pigmentary changes', 'Intellectual disability, FGFR3 mutation, cardiac defects, and pul', 'intellectual disability, fibrosis, ataxia, and pulmonary disease', 'ichthyosis, ataxia, pulmonary dysfunction, and immunodeficit', 'intellectual disability, fibrosis, ataxia, and seizures', 'intellectual disability, fibrosis, alopecia, and pigmentation abnormalities', 'ichthyosis, facial dysmorphism, arthrogryposis, and pul', 'intellectual disability, fragile bones, anxiety, and pulmonary issues']

Singular Values: [122.30469512939453, 114.34846496582031, 82.5096206665039, 71.02500915527344, 61.05084991455078, 55.45585250854492, 55.206974029541016, 45.03531265258789, 5.794018268585205, 1.2034170623171584e-14]

Effective Rank: 7.804594598381604

Eigenscore: -22.963745969679774

E.4 NQ DATASET ON MISTRAL-7B-v0.1

Question: last time east won nba all star game

Correct Answer: ['2014']

LLM's Answer: 2006

Accuracy: 0.0

Sampled Responses: ['2004', '2001', '2001', '2013', '2013', '2013', '2004', '2013']

Singular Values: [1097.43212890625, 585.4111938476562, 355.2393798828125, 2.6302599906921387, 1.0910121140935217e-13, 7.080334175945183e-14, 6.622470177493692e-14, 9.815065427076775e-15, 4.458403975289517e-16, 3.7646645390169164e-30]

Effective Rank: 2.731143238800789

Eigenscore: -61.13279244771307

Question: who was the temple of vesta built for?

Correct Answer: ['Vesta']

LLM's Answer: Vesta

Accuracy: 1.0

Sampled Responses: ['Vesta', 'the goddess vesta', 'Vesta', 'the goddess vesta', 'the goddess vesta', 'Vesta', 'Vesta', 'Vesta', 'Vesta']

Singular Values: [1252.1671752929688, 372.3441772460938, 2.068291691343857e-13, 1.5302303423957858e-13, 1.352673246172607e-14, 2.020799899278259e-29, 9.934199431454563e-30, 4.8484518987236446e-30, 0.0, 0.0]

Effective Rank: 1.7131135330533338

Eigenscore: -62.060661269023285

Question: what percentage of the world died in ww2?

Correct Answer: ['about 3%']

LLM's Answer: 3%

Accuracy: 1.0

Sampled Responses: ['3%', '3%', '3%', '3%', '3%', '3%', '3%', '3%', '3%']

Singular Values: [1136.5360107421875, 3.5605334869695526e-13, 1.574521085343991e-14, 2.644209128265101e-29, 1.6524366075384805e-30, 2.802596928649634e-45, 0.0, 0.0, 0.0, 0.0]

Effective Rank: 1.0000000000000004

Eigenscore: -64.94262853905146

F FURTHER DISCUSSION ON THE EXPERIMENTS

F.1 RELATIONSHIP BETWEEN HALLUCINATION AND UNCERTAINTY

From the above examples, we observe that hallucinations in LLMs are generally positively correlated with their uncertainty. However, counterexamples also exist, such as hallucinated answers with high confidence and correct answers with low confidence. We argue that this phenomenon mainly stems from the diverse causes of hallucination: (i) erroneous internal knowledge, (ii) insufficient internal knowledge and reasoning capability, (iii) excessive stochasticity, and (iv) lack of faithfulness during the generation process. Hallucinations caused by the latter three can often be detected via uncertainty estimation. In contrast, hallucinations due to erroneous internal knowledge are usually associated with low uncertainty, making them difficult to capture with uncertainty-based methods. Therefore, we recommend combining our uncertainty-based approach with knowledge editing and retrieval augmentation techniques to eliminate internal knowledge errors, thereby reducing highly consistent hallucinations and further enhancing AI trustworthiness.

F.2 RELIABILITY AND LIMITATIONS OF ROUGE-L FOR HALLUCINATION ANNOTATION

Based on the case analysis, we find that ROUGE-L is a reliable proxy for hallucination annotation in our experiments, particularly when the dataset contains abundant correct answers and these answers are relatively short. This is because ROUGE-L, by computing the longest common subsequence, effectively checks whether key tokens from the ground-truth answer appear in the model output, similar to keyword-based grading in short-answer exams. In contrast, semantic vector similarity is more prone to misjudgment, as small variations such as additional predicates or modifiers can cause embeddings to be judged as semantically different. Moreover, some questions in our dataset have multiple semantically distinct correct answers, and LLMs may generate multiple answers simultaneously, making semantic similarity metrics less suitable. Another potentially effective annotation method is to determine whether the LLM output and the ground truth are in a bidirectional entailment relationship within context. However, this requires introducing an auxiliary NLI model, which greatly increases annotation complexity. In summary, ROUGE-L aligns well with the characteristics and needs of our datasets and experiments, providing satisfactory annotation reliability. Nevertheless, for more complex scenarios such as multi-turn QA or long-form generation, we recommend adopting more robust hallucination annotation methods.

F.3 TIME COMPLEXITY ANALYSIS OF EFFECTIVE RANK

Although our method requires performing singular value decomposition (SVD) on a matrix composed of multiple high-dimensional vectors, modern libraries such as `numpy.linalg.svd()` make the computation highly efficient. The runtime analysis in the main text (Table 2) shows that the additional computation time of our Effective Rank method is negligible compared to the time required for answer generation. Moreover, its time cost is substantially lower than that of P_False (which introduces extra prompt-based verification) and Semantic Entropy (which requires semantic analysis). For an $m \times n$ matrix with $m < n$, the time complexity of SVD is $\mathcal{O}(m^2n)$. In our main experiments, we compute matrices of size 10×4096 or 50×4096 , where such complexity is entirely acceptable in practice.